## Title

Aging-Related Mitochondrial Dysfunction Is Associated With Fibrosis in Benign Prostatic Hyperplasia.



## Journal

The Journals of Gerontology, Series A: Biological Sciences and Medical Sciences, 79(6)

## Authors

Adrian, Alexis
Liu, Teresa
Pascal, Laura
et al.

## Publication Date

2024-06-01

## DOI

10.1093/gerona/glad222

Peer reviewed

*The Journals of Gerontology, Series A: Biological Sciences and Medical Sciences*, 2024, **79**(6), 1–8
https://doi.org/10.1093/gerona/glad222
Advance access publication 20 September 2023
**Special Issue: Urinary Incontinence and Voiding Dysfunction: Research Article**

# Aging-Related Mitochondrial Dysfunction Is Associated With Fibrosis in Benign Prostatic Hyperplasia

**Alexis E. Adrian, BA,[1] Teresa T. Liu, PhD,[1] Laura E. Pascal, PhD,[2,3] Scott R. Bauer, MD, ScM,[4,5] Donald B. DeFranco, PhD,[2] and William A. Ricke, PhD[1,*]**

[1]Department of Urology, George M. O'Brien Center of Research Excellence, University of Wisconsin—Madison, Madison, Wisconsin, USA.
[2]Department of Pharmacology and Chemical Biology, University of Pittsburgh School of Medicine, Pittsburgh, Pennsylvania, USA.
[3]UPMC Hillman Cancer Center, University of Pittsburgh School of Medicine, Pittsburgh, Pennsylvania, USA.
[4]Department of Medicine, Urology, Epidemiology and Biostatistics, University of California San Francisco, San Francisco, California, USA.
[5]San Francisco VA Medical Center, San Francisco, California, USA.

*Address correspondence to: William A. Ricke, PhD, Department of Urology, University of Wisconsin—Madison, 1111 Highland Ave, 7057 WIMR, Madison, WI 53705, USA. E-mail: rickew@urology.wisc.edu

**Decision Editor**: Roger A. Fielding, PhD, FGSA (Medical Sciences Section)

## Abstract

**Background:** Age is the greatest risk factor for lower urinary tract symptoms attributed to benign prostatic hyperplasia (LUTS/BPH). Although LUTS/BPH can be managed with pharmacotherapy, treatment failure has been putatively attributed to numerous pathological features of BPH (eg, prostatic fibrosis, inflammation). Mitochondrial dysfunction is a hallmark of aging; however, its impact on the pathological features of BPH remains unknown.

**Methods:** Publicly available gene array data were analyzed. Immunohistochemistry examined mitochondrial proteins in the human prostate. The effect of complex I inhibition (rotenone) on a prostatic cell line was examined using quantitative polymerase chain reaction, immunocytochemistry, and Seahorse assays. Oleic acid (OA) was tested as a bypass of complex I inhibition. Aged mice were treated with OA to examine its effects on urinary dysfunction. Voiding was assessed longitudinally, and a critical complex I protein measured.

**Results:** Mitochondrial function and fibrosis genes were altered in BPH. Essential mitochondrial proteins (ie, voltage-dependent anion channels 1 and 2, PTEN-induced kinase 1, and NADH dehydrogenase [ubiquinone] iron–sulfur protein 3, mitochondrial [NDUFS3]) were significantly ($p < .05$) decreased in BPH. Complex I inhibition in cultured cells resulted in decreased respiration, altered NDUFS3 expression, increased collagen deposition, and gene expression. OA ameliorated these effects. OA-treated aged mice had significantly ($p < .05$) improved voiding function and higher prostatic NDUFS3 expression.

**Conclusions:** Complex I dysfunction is a potential contributor to fibrosis and lower urinary tract dysfunction in aged mice. OA partially bypasses complex I inhibition and therefore should be further investigated as a mitochondrial modulator for treatment of LUTS/BPH. Hypotheses generated in this investigation offer a heretofore unexplored cellular target of interest for the management of LUTS/BPH.

**Keywords:** Complex I, Lower urinary tract symptoms, Oxidative phosphorylation, Prostate, Urology

## Background

One in three men over the age of 50 reports bothersome lower urinary tract symptoms (LUTS), a syndrome of overlapping symptoms that occur when storing (eg, urgency, daytime frequency, nocturia, etc.) or voiding urine (eg, weak stream, straining, incomplete voiding, etc.) that significantly reduces the quality of life (1–3). One common driver of LUTS in aging men is benign prostatic hyperplasia (BPH), which affects 50% of men over the age of 50 but dramatically increases to 90% of men by the time they reach their eighties (4–6). In fact, age is the single greatest risk factor for the development of LUTS/BPH. The mechanisms of pathological aging that most directly contribute to the development of LUTS/BPH are yet to be elucidated.

Pharmacologic options for patients with LUTS/BPH are currently limited to 5α-reductase inhibitors, α-blockers, phosphodiesterase-5 inhibitors, or combination therapy (7–9). Surgery is a common outcome for severe or treatment-resistant disease (7–9). The mechanisms contributing to treatment failure or progression of histological BPH to LUTS remain enigmatic. Using prostate samples from a large placebo-controlled randomized clinical trial, we previously demonstrated that total collagen content in the transition zone of the prostate was associated with the risk of clinical progression among men randomly assigned to combination therapy (8). Further preclinical studies in aged mice and other models of lower urinary tract dysfunction (LUTD) have reinforced fibrosis as a driver of LUTS/BPH (10–12).

Although mitochondrial dysfunction is a well-characterized feature of many diseases of aging (13,14) and prostate cancer (15–17), it has not been fully examined in the aging benign prostate. In addition to pathologic aging, mitochondrial dysfunction is also a central mechanistic driver of fibrotic diseases (13,18–21). Oxidative phosphorylation (OXPHOS) is a

Received: April 14 2023; Editorial Decision Date: September 4 2023.

major biochemical function of mitochondria. The reduction in OXPHOS respiration capacity triggers compensatory changes in cellular metabolism, which if maladaptive, can contribute to disease pathology (22–24). OXPHOS generates the majority of adenosine triphosphate (ATP) in the cell, which is used in numerous metabolic reactions and signaling pathways (25). In addition to ATP production, OXPHOS helps maintain the intracellular redox environment, mitochondrial membrane potential, generates reactive oxygen species, and drives most oxygen consumption in cells (23). Many mutations in nuclear and mitochondrial genes encoding components of the electron transport chain (ETC) complexes I–V result in clinical manifestations of disease. Mutations within ETC complex I genes are the most common found in mitochondrial diseases (22), which is likely due to the large number of protein subunits within this complex and the nonoverlapping function of many subunits in its optimal functioning (26). Interestingly, mitochondrial dysfunction, and specifically OXPHOS disruption, is a reputed mechanism contributing to multiple fibrotic diseases (idiopathic pulmonary fibrosis, cardiovascular fibrosis, etc.) (20). However, its contribution to LUTS/BPH remains unexplored.

In this study, we examined the putative relationship between mitochondrial dysfunction, fibrosis, and the aging prostate. Specifically, we explored whether disruption of ETC complex I as a source of mitochondrial dysfunction is associated with prostatic fibrosis. We also tested whether one of the established mitochondrial modulators (ie, oleic acid [OA]) has the capacity to restore mitochondrial bioenergetics and alleviate LUTD in a preclinical aged mouse model.

## Method

### Gene Meta-Analysis

The Tomlins prostate data set (GSE6099) was analyzed using GEO2R to calculate the $p$ values of the 20 000 spotted elements from the Chinnaiyan Human 20K Hs6 cDNA microarray (27). From the data set, there were 28 normal samples and 11 BPH samples. Fold change per gene was calculated as $\Sigma_{BPH}/\Sigma_{normal}$. Genes that had $p$ value less than .05 and fold change greater than 1.5 were input into DAVID (Database for Annotation, Visualization, and Integrated Discover) to assess functional annotations, gene ontology, and pathways.

### Immunohistochemistry

Human prostate samples were from a prostate tissue microarray (pTMA) (12,28,29). The pTMA is made up of 384 duplicate cores from different disease stages (BPH, cancer, etc.), collected from prostatectomy or transurethral resection. For the purposes of this study, the cores examined were benign prostatic tissue (BPT; $n = 48$) and BPH ($n = 24$). All procedures were performed as previously described (30). Briefly, 5-µm sections were cleared and rehydrated through a graded series of ethanol. Antigen retrieval was performed using a Decloaking Chamber (Biocare Medical, Pacheco, CA) in an antigen-retrieval buffer. Sections were stained with anti- voltage-dependent anion channels 1 and 2 (VDAC1/2; Abcam, Cambridge, UK, ab154856, 1:200), anti-PTEN-induced kinase 1 (PINK1; Novus Biologicals, Centennial, CO, NBP1-49678, 1:2000), and anti-NADH dehydrogenase [ubiquinone] iron–sulfur protein 3, mitochondrial (NDUFS3; Thermo Fisher Scientific, Waltham, MA, 459130, 1:200) overnight at 4°C. VDAC1/2 was stained for using DAB (Cell Signaling, Danvers, MA), whereas the OPAL fluorescence kit was used for PINK1 and NDUFS3 (Akoya Biosciences, Marlborough, MA). Mouse prostate samples ($n = 6$, $n = 7$) underwent the same preparation as above, except primary incubation was for 90 minutes at room temperature (OPAL) with anti-NDUFS3 (Proteintech, Rosemont, IL, 15066-1-AP, 1:200). Images were captured using Mantra 2 (Akoya Biosciences) and quantified using InForm software version 2.4.10 (Akoya Biosciences). One 20× image was captured of each pTMA core, whereas 3 representative 20× images were captured for each mouse prostate. Quantification was performed on stroma and epithelial cells, identified via InForm trainable tissue segmentation. The software then performed positivity thresholding and identified the number of positive cells to total cell count (percent positivity). Total tissue percent positivity was determined by averaging epithelial and stromal scores. Fields of view were averaged for each animal before statistical analysis.

### Cell Culture, Treatments, and Reagents

The human prostate stromal (BHPrS1) cell line (31) was grown in RPMI-1640 (Corning, Durham, NC, #10-040-CV) supplemented with 5% fetal bovine serum (Gibco, Grand Island, NY, #10437-010), 0.2% normacin (InvivoGen, San Diego, CA, #ant-nr-1), and 1% HEPES buffer (Corning, #25-060-Cl).

Rotenone (MP Biomedicals, Santa Ana, CA) was solubilized in cell-culture grade dimethyl sulfoxide (DMSO; Sigma, St. Louis, MO). OA (Sigma, #O1383) was solubilized in cell-culture grade ethanol. Methylene blue (Spectrum Chemical Manufacturing Core, Gardena, CA, #M-204) was supplemented in cell-culture media. Cells were treated at 0.1% vehicle (DMSO and ethanol), 25 nM rotenone, 100 nM OA, and 5 ng/mL methylene blue. Reagents for the Seahorse Mito Stress Test were prepared as follows: Oligomycin (Sigma #75351) in methanol, FCCP (Tocris Biosciences, Bristol, UK, #0453) in DMSO, Rotenone (Sigma R8875) in DMSO, and Antimycin A (Sigma A8674) in DMSO.

### Immunocytochemistry

Cells were plated on coverslips in a 6-well plate at $2.5 \times 10^5$ cells per well. After 24 hours, cells were treated and then collected 24 hours after that. Cells were washed and then fixed using 4% paraformaldehyde. After fixation, cells were rinsed, then blocked in 1% normal horse serum, and incubated in primary antibody overnight (Novus, NBP130054, 1:500). After washing, cells were incubated in Donkey anti-Rabbit AlexaFluor 488 (Thermo Fisher Scientific, #A-11008), followed by 4′,6-diamidino-2-phenylindole (DAPI) (Thermo Fisher Scientific, #D1306), and cover slipping. Images were captured on Mantra 2 (Akoya Biosciences), with 5 representative fields of view imaged per treatment. Quantification of the extracellular stain was performed using both the InForm software, to acquire cell counts, and ImageJ to acquire the integrated density for the fluorophore channel (green). The integrated density of a field of view was normalized to the total cell count. Fields of view were averaged for each treatment and biological triplicates were performed.

### RNA Isolation, cDNA Synthesis, and Quantitative Polymerase Chain Reaction

Cells were plated at $1.0 \times 10^5$ cells per well in a 6-well plate. After 24 hours, they were treated. After a 24-hour treatment, cells were collected by cell scraping in PBS. RNA was extracted

from cell pellets using the Promega Maxwell (simply RNA Cells Kit). cDNA synthesis was performed using the iScript cDNA synthesis kit according to manufacturer protocol with 1 µg RNA (BioRad, Hercules, CA). Gene-specific primers were used to validate gene expression (Supplementary Material). Gene expression was normalized to 2 housekeeping genes, YWHAZ and TBP. Biological triplicates were performed.

### Seahorse

BHPrS1 cells were plated at $2.0 \times 10^4$ in the Agilent Seahorse V3-PS tissue culture-treated 96-well plate. Immediately after plating, cells were left at room temperature for 30 minutes. Cells were allowed to adhere for 6 hours and then treated with vehicle (DMSO), 25 nM rotenone, 100 nM OA, or 5 ng/mL methylene blue. Approximately 20 hours after the treatment, cells were switched from RPMI-1640 to unbuffered Dulbecco's Modified Eagle Medium (DMEM) containing 200 mM GlutaMax-1, 100 mM sodium pyruvate, 25 mM glucose, 37 mM NaCl, 42 µM phenol red (pH 7.4). Cells were incubated at 37°C for 1 hour in a $CO_2$-free incubator. A Mito Stress Test was performed with the following assay conditions: 2.5 µM Oligomycin A, 1.4 µM FCCP, 15 µM rotenone, and 10 µM Antimycin A. The plate was mixed and measured 3 times per injection. Biological triplicates were performed.

### Animals

All animal experiments were conducted under the protocols approved by the University of Wisconsin Animal Care and Use Committee. Male C57Bl6/J mice were obtained from The Jackson Laboratory (Strain #000664, Bar Harbor, ME) or directly from the National Institute of Aging (Bethesda, MD). Animals were housed under standard laboratory conditions with 12:12 light/dark cycle and provided with food and water ad libitum. Young mice ($n = 10$) were obtained at 8 weeks of age and aged mice ($n = 19$) were obtained at 24 months of age. Mice treated with OA ($n = 10$) received 30 mg/kg/d of OA in 100 mg of peanut butter, in the form of a pellet, fed daily for 4 weeks. Mice were individually housed during dosing and observed to confirm the dose was consumed, and pellets were consumed within 10 minutes of administration. Mice were euthanized with carbon dioxide/asphyxiation followed by cardiac puncture. Urogenital tracts were dissected, and the mass of anterior prostate (AP) and bladder was determined as previously described (29,32). Tissues for immunohistochemistry (IHC) were fixed in 10% neutral buffered formalin and paraffin embedded.

### Void Spot Assays

Void spot assays (VSAs) were performed as previously described (33). Briefly, mice were placed individually on 16- × 26-cm-thick chromatography paper (Ahlstrom, Kaukauna, WI) in standard mouse cages. Food was provided ad libitum during the 4-hour study, but water was restricted. Filter papers were dried and then imaged with a BioRad ChemiDoc Imaging System under ultraviolet light using an ethidium bromide filter set and 0.5-second exposure (BioRad). Images were imported into ImageJ, color corrected, and void spots analyzed with VoidWhizzard (33).

### Statistics

Comparisons between normal and BPH tissue were made using a 2-sided Student's *t*-test. Quantitative polymerase chain reaction and immunocytochemistry (ICC) were both analyzed using an ordinary 1-way analysis of variance (ANOVA) with the Tukey's correction for multiple comparisons. IHC for mouse AP was analyzed using multiple 1-sided Student's *t*-tests. Seahorse was analyzed using a 1-way ANOVA for each time point. All morphometrics comparing treated and control mice used a 2-sided Student's *t*-test. VSAs were analyzed using multiple 2-sided Student's *t*-test for comparison within pretreatment and separately for pre- to posttreatment VSAs.

### Study Approval

Deidentified human tissue sections were obtained through the University of Wisconsin—Madison. All animal experiments were conducted under the protocols approved by the University of Wisconsin Animal Care and Use Committee.

## Results

### Analysis of Patient Meta-Data Identifies Significantly Altered Genes in the Extracellular Component and Related to Mitochondrial Function

Examination of publicly available microarray data containing normal and BPH prostate samples revealed 121 genes that had significant alterations in expression (Supplementary Material). Pathway analysis showed a significant enrichment in cellular compartment genes that encode for proteins in the extracellular space and tight junctions (Table 1). Upregulated extracellular components related to fibrosis include *ACTA2*, *COL3A1*, *VIM*, and *TGFBR3*. Although mitochondrial genes were not specifically enriched, they represent nearly 10% of genes differentially expressed in normal and BPH prostate tissue ($p$ value = 0.2). Included among these is the essential ETC complex I component, *NDUFS4,* which was downregulated in BPH relative to normal prostate.

### Reduced Accumulation of Various Markers of Mitochondrial Function in BPH Prostate

Using IHC, we measured several known markers of mitochondrial function including VDAC1/2, PINK1, and NDUFS3 (22,34,35). VDAC1/2 is responsible for the movement of metabolites in and out of the mitochondria, while PINK1 is a protein that activates mitophagy in response to mitochondrial dysfunction or damage. Both of these proteins showed decreased expression in prostate stroma and epithelium (Figure 1, Supplementary Material). NDUFS3, a critical protein to complex I assembly and proper electron transport, was also significantly decreased in both prostate epithelium and stroma (Figure 1, Supplementary Material).

### Pharmacologic Inhibition of Complex I in Prostate Stromal Cells Promotes Measures of Fibrosis

In order to determine the potential contribution of complex I disruption to fibrosis, we used the complex I inhibitor, rotenone, in a human prostate stromal cell line (BHPrS1) (36,37). Collagen was used as a marker of fibrosis; extracellular COL1A1 protein expression was increased in rotenone-treated BHPrS1 cells as measured by ICC (Figure 2A). Additionally, *COL1A1* and *COL3A1* gene expression was increased (Figure 2B). To investigate whether these changes were associated with the inhibition of complex I, we measured oxygen consumption rate in rotenone-treated BHPrS1 cells and observed a reduction in respiration measures, especially basal and maximal respiration (Figure 2C). The

**Table 1.** Alterations in Gene Expression of BPH Prostate Samples Compared to Normal Controls Related to the Extracellular Compartment, Tight Junction, and Mitochondria

| Gene Name | BPH vs Normal | *p* Value |
|---|---|---|
| *DDX6* | −378.60 | .05 |
| *VAT1* | −23.55 | .01 |
| *FLNB* | −2.98 | .04 |
| *MAPK8* | −2.97 | .05 |
| *AGK* | −2.91 | .02 |
| *RHOA* | −2.75 | .04 |
| *NDUFS4* | −2.73 | .04 |
| *GNAS* | −2.67 | .02 |
| *PRKAR1A* | −1.95 | .02 |
| *IL1R1* | −1.86 | .00 |
| *NEDD4L* | 25.49 | .01 |
| *IL10RA* | 25.30 | .03 |
| *PLOD3* | 11.69 | .01 |
| *TST* | 11.59 | .00 |
| *PIAS1* | 9.64 | .01 |
| *COL3A1* | 9.46 | .02 |
| *VIM* | 8.76 | .01 |
| *MAPK1* | 5.98 | .00 |
| *GABBR1* | 5.38 | .01 |
| *FBLN1* | 4.87 | .00 |
| *CLDN4* | 4.78 | .00 |
| *FAAH* | 4.40 | .04 |
| *FGFR1* | 4.23 | .00 |
| *MAPK10* | 3.96 | .03 |
| *FBN1* | 3.67 | .01 |
| *CTSL* | 3.66 | .03 |
| *C1R* | 3.49 | .04 |
| *SORBS1* | 2.99 | .04 |
| *CCND2* | 2.95 | .01 |
| *MSN* | 2.86 | .03 |
| *MYL9* | 2.52 | .03 |
| *PTPN11* | 2.44 | .05 |
| *MCL1* | 2.42 | .05 |
| *TGFBR3* | 2.32 | .02 |
| *LAMB2* | 2.32 | .02 |
| *ACTA2* | 2.21 | .04 |
| *ACSS3* | 2.13 | .01 |
| *SGK1* | 2.12 | .04 |

*Note*: BPH = benign prostatic hyperplasia.

inhibitory effects of rotenone on mitochondrial respiration were abated by treatment with methylene blue, a compound used to mitigate complex I inhibition (Figure 2C). The effects of rotenone on respiration were also diminished by cotreatment with OA, an omega-9 fatty acid with known effects that promote OXPHOS function (Figure 2C) (38,39). Notably, OA also reduced the upregulation of collagens I and III gene expression (Figure 2B). Additionally, there was no significant increase in the deposition of extracellular collagen (Figure 2A) in prostate stromal cells treated with rotenone and OA.

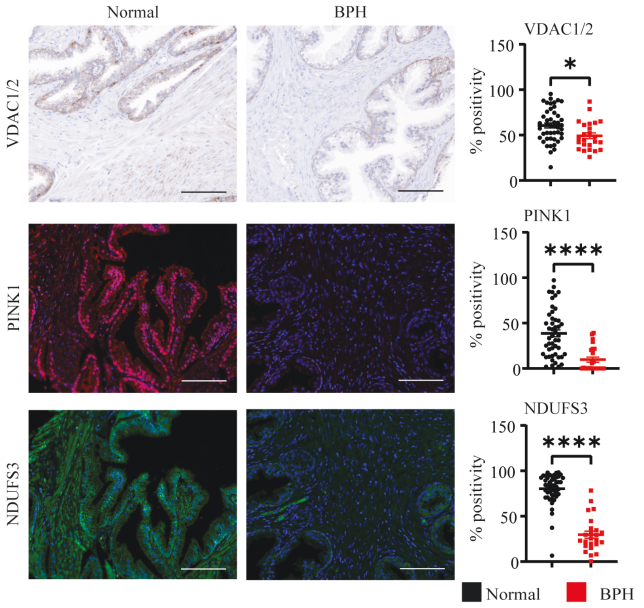


**Figure 1.** Reduced accumulation of various markers of mitochondrial function in BPH prostate. VDAC1/2 (brown), PINK1 (red), and NDUFS3 (green) were all measured using IHC on normal adjacent and BPH prostate tissue samples (BPT = 48, BPH = 24). Using the Inform software, tissues were segmented into epithelial and stroma (Supplementary Material), scored to determine a positivity threshold, and calculated as percent positive of total cells (DAPI). Total expression was calculated by averaging the epithelial and stromal percent positivity of patients. Images were taken at 20× magnification, the scale bar is 100 microns (*$p < .05$; ****$p < .0001$). BPH = benign prostatic hyperplasia; BPT = benign prostatic tissue; IHC = immunohistochemistry; NDUFS3 = NADH dehydrogenase [ubiquinone] iron–sulfur protein 3, mitochondrial; PINK1 = PTEN-induced kinase 1; VDAC1/2 = voltage-dependent anion channels 1 and 2; DAPI = 4′,6-diamidino-2-phenylindole.

### Oleic Acid Treatment Significantly Improves Voiding Dysfunction and Complex I Impairment in Aged Mice

We have previously shown that aged mice (24 months) develop voiding dysfunction and other hallmarks of LUTD compared to young (2-month) mice (40,41). To determine if aged mice also have a reduction in complex I function, we performed IHC for NDUFS3 on mouse prostate, and saw a significant ($p < .05$) decrease in its accumulation in the AP (Figure 3A). To evaluate the effectiveness of OA in rescuing both mitochondrial-complex I function and urinary dysfunction, aged mice were fed OA daily for 4 weeks. After euthanasia, mouse urogenital tracts (UGTs) were dissected (Figure 3B). OA had no significant effect on body weight, measured immediately after euthanasia (Figure 3C). Bladder mass was significantly decreased (Figure 3D), but AP was not significantly altered (Figure 3E). Aged mice also showed a significant improvement in voiding dysfunction (ie, decreased frequency) as assessed by VSA after OA treatment which was not observed in untreated controls (Figure 3F). Complex I function was also partially restored, as perceived by increased NDUFS3 expression in OA-treated aged mice (Figure 3A).

## Discussion

Mitochondrial dysfunction is a fundamental contributor to aging and many aging-related pathologies; this study investigated whether mitochondrial dysfunction occurs in the

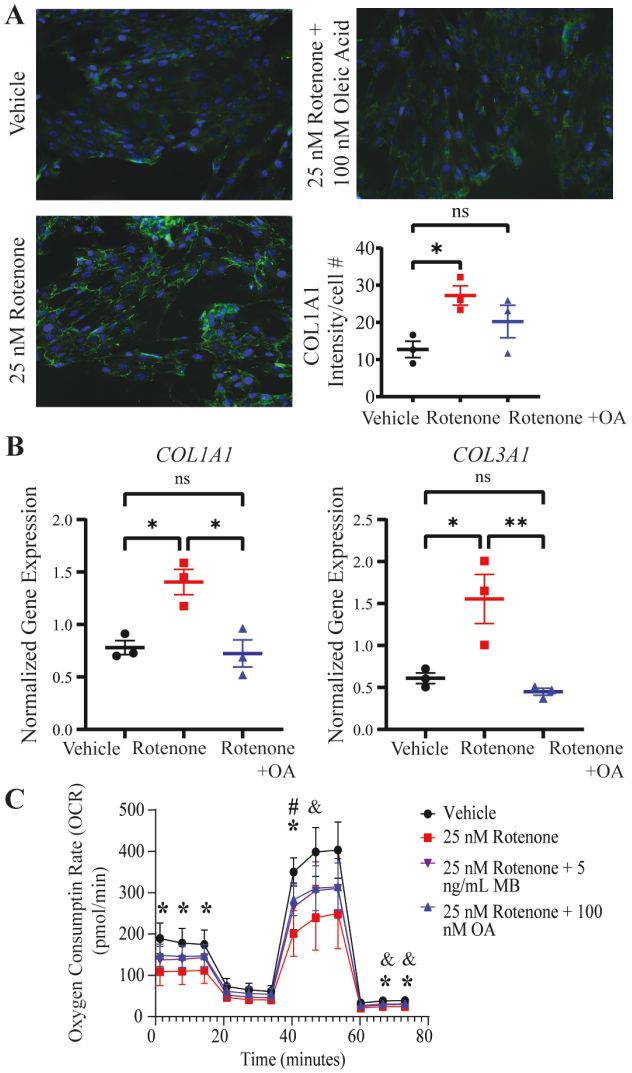


**Figure 2.** Pharmacologic inhibition of complex I in prostate stromal cells promotes measures of fibrosis. Inhibition of complex I results in increased collagen expression and decreased cellular respiration. (A) ICC analysis of extracellular COL1A1 (green) was increased in 25 nM rotenone-treated BHPrS1 cells, an increase that was not seen when 100 nM oleic acid was also present. Nuclei were stained with DAPI (blue). Images were taken at 20× magnification. Green intensity was measured in ImageJ and normalized to the number of cells per field of view (*$p < .05$). (B) COL1A1 and COL3A1 gene expression was upregulated in rotenone-treated BHPrS1 cells and this was mitigated by 100 nM oleic acid as determined by qPCR (*$p < .05$, **$p < .01$, ns, not significant). (C) Seahorse mito stress test analysis of BHPrS1 cells showed a decrease in oxygen consumption rate for rotenone-treated cells, which was mitigated by methylene blue (MB). Oleic acid was able to mitigate the decrease as effectively as methylene blue, the known bypass agent (*$p < .05$ for DMSO vs 25 nM rotenone, #$p < .05$ for DMSO vs 25 nM rotenone + 100 nM oleic acid, & $p < .05$ for DMSO vs 25 nM Rotenone + 5 ng/mL MB). DMSO = dimethyl sulfoxide; ICC = immunocytochemistry; DAPI = 4′,6-diamidino-2-phenylindole.

prostate of men with LUTS/BPH and an aged mouse model. Collectively, these data identified indications of mitochondrial dysfunction in patient samples and an aged mouse model of LUTD, as well as identifying an in vitro model linking OXPHOS disruption to increased collagen expression. Analysis of publicly available prostate data revealed significant changes in the expression of genes in fibrotic pathways

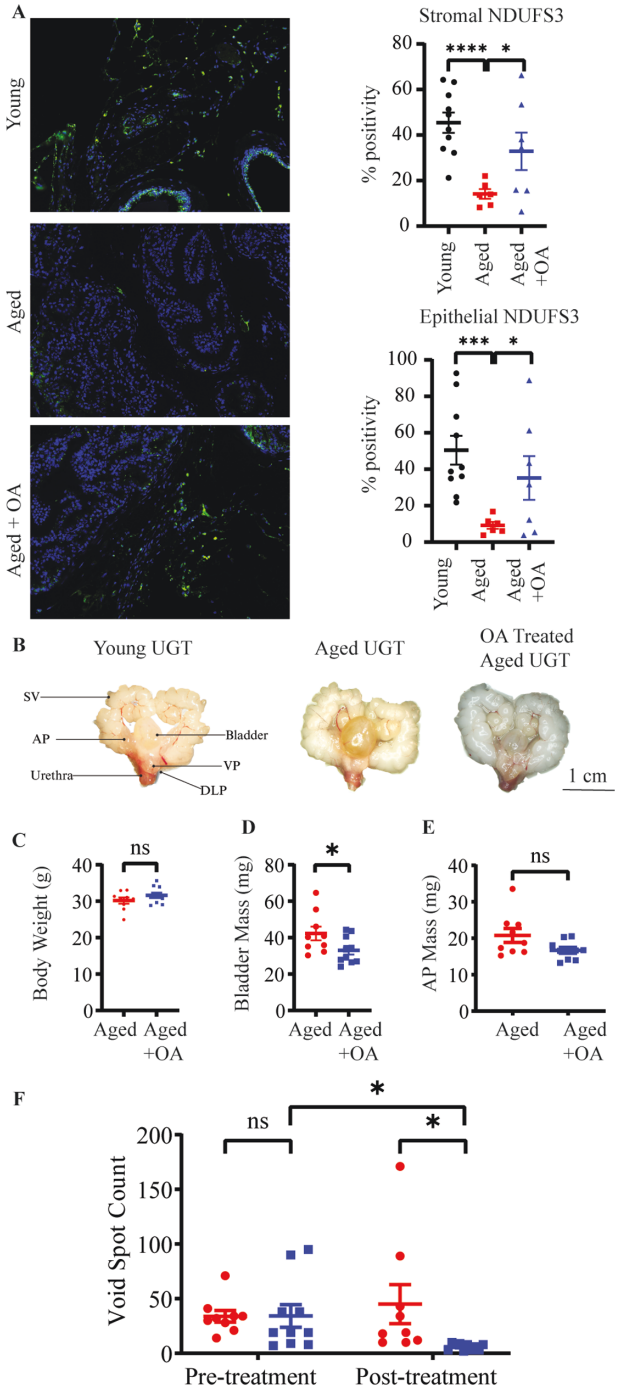


**Figure 3.** Oleic acid mitigates mitochondrial and urinary dysfunction seen in aged mice. (A) Percent positive NDUFS3 (green), cells a complex I marker, was decreased in aged mouse anterior prostate (A). This change was partially rescued by a 4-week treatment of oleic acid. (B) Images of the urogenital tract of young, aged, and oleic-acid-treated aged mice. (C) Oleic acid treatment did not affect the body weight at the time of euthanasia. (D) Bladder mass was significantly decreased in oleic acid treated mice. (E) Anterior prostate mass was not significantly altered in the oleic acid treated mice. (F) Void spot count was not different between the aged mice prior to treatment. After treatment, void spot count was significantly different between the treated and untreated group, as well as comparing the pretreatment and posttreatment counts of the oleic-acid-treated mice (*$p < .05$, ***$p < .001$, ns, not significant). AP = anterior prostate; DLP = dorsolateral prostate; SV = seminal vesicles; VP = ventral prostate; UGT = urogenital tract.

(*COL3A1*, *TGFBR3)* and at least 1 component of ETC complex I (*NDUFS4)*. Using IHC to assess protein accumulation, we observed a decrease in 2 distinct markers of mitochondrial function (VDAC1/2 and PINK1) in prostates of BPH patients relative to normal specimens (42,43). VDAC1/2 are mitochondrial membrane proteins, with VDAC1 being the most abundant protein in the mitochondrial outer membrane (34). VDAC1 also acts as a gatekeeper of ions and metabolites, which is critical in the regulation of mitochondrial metabolism (34). PINK1, which has been demonstrated to directly interact with OXPHOS components, is primarily a mitophagy protein, promoting clearance of defective or damaged mitochondria (44,45). Moreover, NDUFS3 was also decreased in BPH tissue. NDUFS3 is a critical component of the catalytic action of complex I in addition to being necessary for assembly (22). A decrease in the expression of NDUFS3 is an indicator of decreased complex I function, which may limit mitochondrial OXPHOS and other pathways. Collectively, these data indicate the presence of mitochondrial dysfunction in the prostate of men with LUTS/BPH, thus identifying a heretofore unexplored cellular target of interest for the management of LUTS/BPH.

Pharmacologic inhibition of complex I resulted in increased *COL3A1* gene expression and increased COL1A1 at the gene and protein levels. Respirometry of rotenone-treated prostate stromal cells demonstrated a clear decrease in OXPHOS respiration, confirming OXPHOS-driven respiration is active in these cells. Notably, methylene blue ameliorated the decreased oxygen consumption caused by rotenone, as expected given studies showing its ability to mitigate inhibition by rotenone (46). Interestingly, OA similarly improved respiration inhibition caused by rotenone, identifying it as a putative bypass agent for complex I dysfunction. OA also ameliorated the increased collagen gene and protein expression, demonstrating it may be a potential antifibrotic and mitochondrial modulator to test in preclinical models. The association seen between mitochondrial dysfunction and fibrosis in other diseases is recapitulated in a prostate stromal cell line model of complex I dysfunction.

The aged mouse model of LUTD recapitulates complex I dysfunction observed in patient samples, as demonstrated by a decrease in NDUFS3 in the AP. Furthermore, treatment of aged mice with OA significantly improved NDUFS3 expression in the AP. Additionally, OA treatment ameliorated voiding dysfunction, as measured by void spot count, suggesting that maintaining mitochondrial-complex I function may be required for optimal lower urinary tract function, particularly in aged animals. While OA has been shown to work directly on OXPHOS, it also has properties as an antioxidant and anti-inflammatory agent (38,39). Thus, the contributions of other cellular or systemic protective effects of OA beyond the restoration of mitochondrial function to the resolution of aging-dependent LUTD in mice remain to be determined. Furthermore, the aged mouse model is not exclusively a model of mitochondrial dysfunction, which is a limitation in identifying the direct mechanism of action. Further work is necessary using loss-of-function models to better understand the connection between OXPHOS disruption, mitochondrial dysfunction, and processes associated with the development of LUTS/BPH.

Collectively, this investigation generates a new pathway of interest for the aging prostate as it relates to the development of LUTS/BPH. Specifically, we provide evidence for mitochondrial dysfunction in prostate tissue from patients with LUTS/BPH and an aged mouse model, as well as evidence of potential amelioration of OXPHOS disruption and LUTD by OA. In addition, an association between complex I disruption and increased collagen production was observed in a human prostate stromal cell line. Additional patient samples are needed to further characterize disease-specific changes potentially present in mitochondria and to determine if associations from cell lines extend to patients with LUTS/BPH, or a subset thereof. More specific mouse models are also required to elucidate a possible mechanism driving mitochondrial dysfunction in the prostate, as well as evaluate the potential of new therapeutics and supplements for treating LUTS/BPH, such as OA. Ultimately, mitochondria are a promising new target for addressing the treatment failures experienced by many LUTS/BPH patients.

## Supplementary Material

Supplementary data are available at *The Journals of Gerontology, Series A: Biological Sciences and Medical Sciences* online.

## Funding

This work was supported by the National Institutes of Health (T32GM141013andF31DK136335toA.E.A.,K01AG059899 to T.T.L., R03 AG067937 and K76 AG074903 to S.R.B., U54 DK104310, R01 DK131175, and R01 DK127081 to W.A.R.). This work was also supported by funding from Collaborating for the Advancement of Interdisciplinary Research in Benign Urology (CAIRIBU) (Convergence Award to LEP and Opportunity Pool award to SRB). Seahorse experiments were performed with funding from the University of Wisconsin Carbone Cancer Center Support Grant P30CA014520.

## Conflict of Interest

None.

## Acknowledgments

We would like to thank the members of the Ricke Lab for their help and support. We would like to thank Gene Ananiev and the UW—Madison Small Molecule Screening Facility for the use of their Agilent Seahorse instrument and experimental support. We would also like to thank Dr. Sruti Shiva and Dr. Courtney Watkins for their expertise on Seahorse experiments.

## Author Contributions

A.E.A., T.T.L., L.E.P., D.B.D., and W.A.R. contributed to the development of the project. All authors contributed equally to the revision of the manuscript. A.E.A. and T.T.L. performed the experiments and data analysis.

## References

1. Wei JT, Calhoun E, Jacobsen SJ. Urologic diseases in America project: benign prostatic hyperplasia. *J Urol.* 2005;173:1256–1261. https://doi.org/10.1097/01.ju.0000155709.37840.fe

2. Girman CJ, Jacobsen SJ, Tsukamoto T, et al. Health-related quality of life associated with lower urinary tract symptoms in four countries. *Urology*. 1998;51:428–436. https://doi.org/10.1016/s0090-4295(97)00717-6
3. Taylor BC, Wilt TJ, Fink HA, et al.; Osteoporotic Fractures in Men (MrOS) Study Research Group. Prevalence, severity, and health correlates of lower urinary tract symptoms among older men: the MrOS study. *Urology*. 2006;68:804–809. https://doi.org/10.1016/j.urology.2006.04.019
4. Garraway WM, Collins GN, Lee RJ. High prevalence of benign prostatic hypertrophy in the community. *Lancet*. 1991;338:469–471. https://doi.org/10.1016/0140-6736(91)90543-x
5. Jacobsen SJ, Jacobson DJ, Girman CJ, et al. Treatment for benign prostatic hyperplasia among community dwelling men: the Olmsted County Study of Urinary Symptoms and Health Status. *J Urol*. 1999;162:1301–1306.
6. Berry SJ, Coffey DS, Walsh PC, Ewing LL. The development of human benign prostatic hyperplasia with age. *J Urol*. 1984;132:474–479. https://doi.org/10.1016/s0022-5347(17)49698-4
7. Bautista OM, Kusek JW, Nyberg LM, et al. Study design of the Medical Therapy of Prostatic Symptoms (MTOPS) trial. *Control Clin Trials*. 2003;24:224–243. https://doi.org/10.1016/s0197-2456(02)00263-5
8. Macoska JA, Uchtmann KS, Leverson GE, McVary KT, Ricke WA. Prostate transition zone fibrosis is associated with clinical progression in the MTOPS study. *J Urol*. 2019;202:1240–1247. https://doi.org/10.1097/JU.0000000000000385
9. McConnell JD, Roehrborn CG, Bautista OM, et al.; Medical Therapy of Prostatic Symptoms (MTOPS) Research Group. The long-term effect of doxazosin, finasteride, and combination therapy on the clinical progression of benign prostatic hyperplasia. *N Engl J Med*. 2003;349:2387–2398. https://doi.org/10.1056/NEJMoa030656
10. Ricke WA, Bruskewitz RC, Liu TT. Targeting a fibrotic bottleneck may provide an opening in the treatment of LUTS. *Am J Physiol Renal Physiol*. 2019;316:F1091–F1093. https://doi.org/10.1152/ajprenal.00102.2019
11. Drifka CR, Loeffler AG, Mathewson K, et al. Comparison of picrosirius red staining with second harmonic generation imaging for the quantification of clinically relevant collagen fiber features in histopathology samples. *J Histochem Cytochem*. 2016;64:519–529. https://doi.org/10.1369/0022155416659249
12. Bauman TM, Nicholson TM, Abler LL, et al. Characterization of fibrillar collagens and extracellular matrix of glandular benign prostatic hyperplasia nodules. *PLoS One*. 2014;9:e109102. https://doi.org/10.1371/journal.pone.0109102
13. Cui H, Kong Y, Zhang H. Oxidative stress, mitochondrial dysfunction, and aging. *J Signal Transduct*. 2012;2012:646354. https://doi.org/10.1155/2012/646354
14. Amorim JA, Coppotelli G, Rolo AP, Palmeira CM, Ross JM, Sinclair DA. Mitochondrial and metabolic dysfunction in ageing and age-related diseases. *Nat Rev Endocrinol*. 2022;18:243–258. https://doi.org/10.1038/s41574-021-00626-7
15. Dakubo GD, Parr RL, Costello LC, Franklin RB, Thayer RE. Altered metabolism and mitochondrial genome in prostate cancer. *J Clin Pathol*. 2006;59:10–16. https://doi.org/10.1136/jcp.2005.027664
16. Hopkins JF, Sabelnykova VY, Weischenfeldt J, et al. Mitochondrial mutations drive prostate cancer aggression. *Nat Commun*. 2017;8:656. https://doi.org/10.1038/s41467-017-00377-y
17. Guerra F, Guaragnella N, Arbini AA, Bucci C, Giannattasio S, Moro L. Mitochondrial dysfunction: a novel potential driver of epithelial-to-mesenchymal transition in cancer. *Front Oncol*. 2017;7:295. https://doi.org/10.3389/fonc.2017.00295
18. Lopez-Otin C, Blasco MA, Partridge L, Serrano M, Kroemer G. The hallmarks of aging. *Cell*. 2013;153:1194–1217. https://doi.org/10.1016/j.cell.2013.05.039
19. Berry BJ, Kaeberlein M. An energetics perspective on geroscience: mitochondrial protonmotive force and aging. *Geroscience*. 2021;43:1591–1604. https://doi.org/10.1007/s11357-021-00365-7
20. Li X, Zhang W, Cao Q, et al. Mitochondrial dysfunction in fibrotic diseases. *Cell Death Discov*. 2020;6:80. https://doi.org/10.1038/s41420-020-00316-9
21. Pieczenik SR, Neustadt J. Mitochondrial dysfunction and molecular pathways of disease. *Exp Mol Pathol*. 2007;83:84–92. https://doi.org/10.1016/j.yexmp.2006.09.008
22. Fassone E, Rahman S. Complex I deficiency: clinical features, biochemistry and molecular genetics. *J Med Genet*. 2012;49:578–590. https://doi.org/10.1136/jmedgenet-2012-101159
23. Smeitink JA, Zeviani M, Turnbull DM, Jacobs HT. Mitochondrial medicine: a metabolic perspective on the pathology of oxidative phosphorylation disorders. *Cell Metab*. 2006;3:9–13. https://doi.org/10.1016/j.cmet.2005.12.001
24. Zielinski LP, Smith AC, Smith AG, Robinson AJ. Metabolic flexibility of mitochondrial respiratory chain disorders predicted by computer modelling. *Mitochondrion*. 2016;31:45–55. https://doi.org/10.1016/j.mito.2016.09.003
25. Wilson DF. Oxidative phosphorylation: regulation and role in cellular and tissue metabolism. *J Physiol*. 2017;595:7023–7038. https://doi.org/10.1113/JP273839
26. Sharma LK, Lu J, Bai Y. Mitochondrial respiratory complex I: structure, function and implication in human diseases. *Curr Med Chem*. 2009;16:1266–1277. https://doi.org/10.2174/092986709787846578
27. Tomlins SA, Mehra R, Rhodes DR, et al. Integrative molecular concept modeling of prostate cancer progression. *Nat Genet*. 2007;39:41–51. https://doi.org/10.1038/ng1935
28. Huang W, Hennrick K, Drew S. A colorful future of quantitative pathology: validation of Vectra technology using chromogenic multiplexed immunohistochemistry and prostate tissue microarrays. *Hum Pathol*. 2013;44:29–38. https://doi.org/10.1016/j.humpath.2012.05.009
29. Nicholson TM, Moses MA, Uchtmann KS, et al. Estrogen receptor-alpha is a key mediator and therapeutic target for bladder complications of benign prostatic hyperplasia. *J Urol*. 2015;193:722–729. https://doi.org/10.1016/j.juro.2014.08.093
30. Nicholson TM, Sehgal PD, Drew SA, Huang W, Ricke WA. Sex steroid receptor expression and localization in benign prostatic hyperplasia varies with tissue compartment. *Differentiation*. 2013;85:140–149. https://doi.org/10.1016/j.diff.2013.02.006
31. Franco OE, Jiang M, Strand DW, et al. Altered TGF-beta signaling in a subpopulation of human stromal cells promotes prostatic carcinogenesis. *Cancer Res*. 2011;71:1272–1281. https://doi.org/10.1158/0008-5472.CAN-10-3142
32. Nicholson TM, Ricke EA, Marker PC, et al. Testosterone and 17beta-estradiol induce glandular prostatic growth, bladder outlet obstruction, and voiding dysfunction in male mice. *Endocrinology*. 2012;153:5556–5565. https://doi.org/10.1210/en.2012-1522
33. Wegner KA, Abler LL, Oakes SR, et al. Void spot assay procedural optimization and software for rapid and objective quantification of rodent voiding function, including overlapping urine spots. *Am J Physiol Renal Physiol*. 2018;315:F1067–F1080. https://doi.org/10.1152/ajprenal.00245.2018
34. Camara AKS, Zhou Y, Wen PC, Tajkhorshid E, Kwok WM. Mitochondrial VDAC1: a key gatekeeper as potential therapeutic target. *Front Physiol*. 2017;8:460. https://doi.org/10.3389/fphys.2017.00460
35. Matsuda S, Kitagishi Y, Kobayashi M. Function and characteristics of PINK1 in mitochondria. *Oxid Med Cell Longev*. 2013;2013:601587. https://doi.org/10.1155/2013/601587
36. Palmer G, Horgan DJ, Tisdale H, Singer TP, Beinert H. Studies on the respiratory chain-linked reduced nicotinamide adenine dinucleotide dehydrogenase. *J Biol Chem*. 1968;243:844–847. https://doi.org/10.1016/s0021-9258(19)81742-8
37. Singer TP, Ramsay RR. The reaction sites of rotenone and ubiquinone with mitochondrial NADH dehydrogenase. *Biochim Biophys Acta*. 1994;1187:198–202. https://doi.org/10.1016/0005-2728(94)90110-4
38. Pompura SL, Wagner A, Kitz A, et al. Oleic acid restores suppressive defects in tissue-resident FOXP3 Tregs from patients with

multiple sclerosis. *J Clin Invest*. 2021;131:e138519. https://doi.org/10.1172/JCI138519
39. Matsuoka I, Nakamura T. Reversible effects of fatty acids on respiration, oxidative phosphorylation, and heat production of rat liver mitochondria. *J Biochem*. 1979;86:675–681. https://doi.org/10.1093/oxfordjournals.jbchem.a132571
40. Liu TT, Thomas S, Mclean DT, et al. Prostate enlargement and altered urinary function are part of the aging process. *Aging (Milano)*. 2019;11:2653–2669. https://doi.org/10.18632/aging.101938
41. Pascal LE, Igarashi T, Mizoguchi S, et al. E-cadherin deficiency promotes prostate macrophage inflammation and bladder overactivity in aged male mice. *Aging (Albany NY)*. 2022;14:2945–2965. https://doi.org/10.18632/aging.203994
42. Ham SJ, Lee D, Yoo H, Jun K, Shin H, Chung J. Decision between mitophagy and apoptosis by Parkin via VDAC1 ubiquitination. *Proc Natl Acad Sci U S A*. 2020;117:4281–4291. https://doi.org/10.1073/pnas.1909814117
43. Geisler S, Holmstrom KM, Skujat D, et al. PINK1/Parkin-mediated mitophagy is dependent on VDAC1 and p62/SQSTM1. *Nat Cell Biol*. 2010;12:119–131. https://doi.org/10.1038/ncb2012
44. Liu W, Acin-Perez R, Geghman KD, Manfredi G, Lu B, Li C. Pink1 regulates the oxidative phosphorylation machinery via mitochondrial fission. *Proc Natl Acad Sci U S A*. 2011;108:12920–12924. https://doi.org/10.1073/pnas.1107332108
45. Pickrell AM, Youle RJ. The roles of PINK1, Parkin, and mitochondrial fidelity in Parkinson's disease. *Neuron*. 2015;85:257–273. https://doi.org/10.1016/j.neuron.2014.12.007
46. Xue H, Thaivalappil A, Cao K. The potentials of methylene blue as an anti-aging drug. *Cells*. 2021;10:3379. https://doi.org/10.3390/cells10123379